Fuel, Volume 101, November 2012, Pages 115–128

Elsevier Editorial System(tm) for Fuel
Manuscript Draft

Manuscript Number:

Title: Demonstrating full-scale post-combustion CO2 capture for coal-fired power plants through dynamic modelling and simulation

Article Type: Special Issue: 8th ECCRIA

Keywords: Post-combustion CO2 capture; coal-fired power plant; flexibility; dynamic modelling; simulation; scale-up

Corresponding Author: Dr Meihong WANG, PhD, MSc, CEng

Corresponding Author's Institution: Cranfield University

First Author: Adekola Lawal, MSc BSc

Order of Authors: Adekola Lawal, MSc BSc; Meihong WANG, PhD, MSc, CEng; Peter Stephenson, PhD CEng BSc ; Okwose Obi, MSc BSc

Abstract: This study seeks to provide insights into the design and operation of full-scale post-combustion CO2 capture for a 500MWe subcritical power plant through dynamic modelling and simulation. The development and validation of the dynamic models of the power plant and CO2 capture plant is described. In addition, the scale-up of the CO2 capture plant from pilot plant scale (where it was validated) to full scale is discussed. Subsequently the manner in which the two plant models were linked is discussed. A floating IP/LP crossover pressure configuration is used. A throttling valve is included between the LP turbine and draw-off point to prevent pressures at the crossover from dropping below required levels in the reboiler for solvent regeneration. The flue gas from the power plant is treated before it is sent to the CO2 capture plant. Four case studies are considered. The first investigates the effect of increasing solvent concentration on the performance of the whole plant. The second investigates which absorber packing height offers a good balance between capital and operating costs. The two dynamic case studies show that the CO2 capture plant has a slower response than the power plant. They also reveal an interaction of CO2 capture level and power plant output control loops making it difficult to achieve steady power output levels quickly.

Suggested Reviewers: Robert M Davidson
Head of Coal Science and Information Services, IEA Clean Coal Centre
robert@iea-coal.org.uk
Mr Robert M Davidson from IEA Clean Coal Centre is an expert in this area.

David Mcilveen-Wright PhD
Lecturer, Ulster University
dr.mcilveen-wright@ulster.ac.uk
Dr David Mcilveen-Wright is an expert in modelling and simulation for energy systems including various power plants.

Hanne M Kvamsdal PhD
Research Scientist, Materials and Chemistry, Process Technology , SINTEF, Norway
Hanne.Kvamsdal@sintef.no

Dr Hanne Marie Kvamsdal is an expert in modelling and simulation for carbon capture.

Manuscript
Click here to view linked References

Demonstrating full-scale post-combustion CO_2 capture for coal-fired power plants through dynamic modelling and simulation

Adekola Lawal[a], Meihong Wang[a*] , Peter Stephenson[b], Okwose Obi[a]

[a]*Process Systems Engineering Group, School of Engineering, Cranfield University, UK, MK43 0AL*

[b]*RWE npower, Windmill Hill Business Park, Swindon, UK, SN5 6PB*

Abstract

This study seeks to provide insights into the design and operation of full-scale post-combustion CO_2 capture for a 500MWe subcritical power plant through dynamic modelling and simulation. The development and validation of the dynamic models of the power plant and CO_2 capture plant is described. In addition, the scale-up of the CO_2 capture plant from pilot plant scale (where it was validated) to full scale is discussed. Subsequently the manner in which the two plant models were linked is discussed. A floating IP/LP crossover pressure configuration is used. A throttling valve is included between the LP turbine and draw-off point to prevent pressures at the crossover from dropping below required levels in the reboiler for solvent regeneration. The flue gas from the power plant is treated before it is sent to the CO_2 capture plant. Four case studies are considered. The first investigates the effect of increasing solvent concentration on the performance of the whole plant. The second investigates which absorber packing height offers a good balance between capital and operating costs. The two dynamic case studies show that the CO_2 capture plant has a slower response than the power plant. They also reveal an interaction of CO_2 capture level and power plant output control loops making it difficult to achieve steady power output levels quickly.

Keywords: Post-combustion CO_2 capture; coal-fired power plant; flexibility; dynamic modelling; simulation; scale-up

1. Introduction

1.1 Background

Chemical absorption of CO_2 using MEA solvent has been recommended as a suitable technology for post-combustion plants especially for retrofit purposes. Although the process technology has been applied in natural gas sweetening, the scale of process required to achieve up to 90% CO_2 capture in fossil fuel-fired power plants is

[*] *Corresponding author. Tel: +0044 1234 754655; Fax: +0044 1234 754685; Email address: meihong.wang@cranfield.ac.uk*

typically several times larger than what is commercially available at present. For instance Mitsubishi Heavy Industries (MHI) has built some of the largest plants that process up to 450 tonnes of CO_2 per day from natural gas fired boilers [1]. A 500MWe supercritical coal-fired power plant operating at 46% efficiency (LHV basis) [2] would release over 8000tonnes of CO_2 per day. To separate CO_2 from flue gas at that scale, a relatively large chemical absorption facility is required which would be a significant capital investment to the operator.

The operation of a power plant integrated with a chemical absorption process would present additional challenges. The efficiency of such plants would drop significantly because steam that would have been used to generate electricity is drawn off to regenerate the solvent. Several studies have demonstrated that significant energy penalties would be incurred with the inclusion of carbon capture technology [3-5]. In addition, resultant reduced steam flows to the low pressure (LP) turbines would ultimately result in reduced pressures upstream of this point in the turbine. This and the possible process modifications required are described in the study. Another concern is whether such power plants could continue to play their role in meeting electricity demand. Coal-fired power plants currently operate flexibly in meeting varying electricity demand. Having power generation processes that could operate flexibly would be increasingly important with the growth of renewable power generation. Though renewable sources are virtually carbon neutral, they suffer the drawback of being intermittent in nature. Such variations in power generation increase the requirement for flexible operation in other plants on the same electricity grid. Hence both the coal-fired power plant itself and the downstream CO_2 chemical absorption process would have to be capable of flexible operation.

1.2 Motivation

Design and operational studies are typically carried out with pilot and larger scale demonstration plants. Current pilot plant studies worldwide are on a much smaller scale than would be required for CCS. Even at such scales (typically less than 5MWe), the cost of construction for these facilities typically runs up to several million dollars [6]. Once built, these plants are limited in the range of studies that could be carried out. Full scale demonstration projects are estimated to cost over a billion dollars [6]. A lot of useful insights could be derived from accurate dynamic models of the post-combustion capture process at a much lower cost.

Most process models developed to study cost and performance implications of CCS have been steady state models which cannot account for the various transients associated in the power generation process. Transients occur during plant start-up and shutdown operations. Load-following operations are common in coal-fired power plants. Operational problems could be further compounded if there are tight restrictions on CO_2 emissions. The downstream

absorption plant may have to closely follow load changes. Finally, to improve overall efficiency, increased process integration of the power generation process and capture process would be required. This would likely further complicate the operation of the integrated facility. Insights regarding the integrated plant operation could also be provided through studies using dynamic modelling and simulation.

1.3 Previous Research

A number of studies have been carried out on dynamic model development of the chemical absorption plant. [7] and [8] present the dynamic model development and simulation of the absorber only. [8] also discusses different types of models used for modelling reactive absorption and the developments made in this regard. Rate-based models are shown to be more accurate than equilibrium-based ones. [9] describes the dynamic model development and simulation of the regenerator only while [10] extends this to the two stand-alone absorber and regenerator column models Analysis on stand-alone columns may be inaccurate due to the inevitable coupling of the two columns linked with a recycle loop. [11] describes the dynamic model development of the chemical absorption process (absorber and regenerator linked by recycling the solvent). This model, however, was developed and validated at pilot plant scale, three orders of magnitude smaller than what is required for processing flue gas from a coal-fired power plant generating 500MWe. [12] investigated the performance and dynamic response of the chemical absorption process downstream an enhanced oxygen coal power plant and demonstrated how there was room for further improvement of performance by addressing the increased absorber temperatures.

A number of studies explored the dynamic response of power plants. [13] combined a dynamic model with steady state correlations to simulate power plant component dynamics in MATLAB/SIMULINK. The components could be linked to form a power plant. The dynamic model developed was not validated though some simulation results for a whole plant were shown. [14] derived a model from first principles to describe the drum, downcomer, and riser components of a natural circulation drum-boiler. [15] modelled from first principles a 250MW coal-fired natural circulation boiler. The boiler system was divided into seven submodels: downcomer, riser, waterwall, drum, superheater and reheater, attemperator, and furnace. [16] developed a dynamic model of a sub-critical once-through Benson type boiler based on the experimental data obtained from a complete set of field experiments. Genetic algorithm (GA) was executed to estimate the model parameters and fit the models response on the real system dynamics. [17] developed dynamic models of a subcritical coal-fired power plant in gPROMS and validated the results with plant data. These power plant models described by these authors do not include integration with a CO_2 capture plant.

Steady state models of the CO_2 capture plant integrated with the power plant have been developed. A steady state, in-house model was used by [18] to compare the performance of different process configurations and different solvents (including solvent blends) for the chemical absorption plant integrated with a supercritical power plant. [19] carried out a study of the integration of the two plants using a steady state model. The model also considered CO_2 compression. Another steady state integration study was carried out by [20]. In this study, the impact of CO_2 compression was considered as well and efficiency penalties estimated were up to 16%.

1.4 Scope of the study and novelties of the paper

This study was conducted with a modelling and simulation approach. The gPROMS (Process Systems Enterprise Ltd.) advanced process modelling environment has been used to implement the proposed work. Dynamic models of the CO_2 chemical absorption and power generation processes were developed for a 500MWe subcritical coal-fired power plant. A subcritical plant was used and not supercritical one because there was plant data available for dynamic validation obtained from one of the plants RWE npower operates. The two dynamic process models were linked together to carry out a unique study of their integrated operation.

2. CO_2 capture model development and validation

Rate-based dynamic models of the CO_2 absorption process consist mainly of the absorber and regenerator column model. Mass transfer rates in the columns were modelled based on the two-film theory using the Maxwell-Stefan formulation while the reactions were assumed to attain equilibrium. Dynamic validation of the CO_2 absorption model was carried out at pilot plant scale. The model was subsequently scaled up to full scale and therefore able to process the flue gas from a 500MWe subcritical power plant.

2.1 Model assumptions

The following assumptions were used in developing this dynamic model:

a. All reactions are assumed to attain equilibrium
b. Plug flow regime and linear pressure drop along the column
c. Phase equilibrium at interface between liquid and vapour films
d. Negligible holdup in the vapour bulk
e. Negligible solvent degradation
f. Negligible heat loss in the absorber column

2.2 Model Equations

The amine plant consists of two main packed columns – the absorber and regenerator. More details of the absorber

and regenerator dynamic model are described in [11]. In the packed column section, the main models include the vapour and liquid bulk models, the vapour and liquid film models and the interface (Figure 1).

The main equations are listed for the convenience of readers.

For the liquid bulk, the mass and energy balance equations are listed.

Mass Balance: $$\frac{dM_i}{dt} = \frac{-1}{L \cdot A}\frac{\partial F_i^L}{\partial y} + N_i \cdot Sp \cdot MW_i \cdot \omega \quad (1)$$

Energy Balance: $$\frac{dU}{dt} = \frac{-1}{L \cdot A}\frac{\partial F_H^L}{\partial y} + Sp \cdot \omega \cdot \left(H_{liq}^{cond} + H_{liq}^{conv} + H_{abs}\right) + HL \quad (2)$$

The change in component mass holdup, M_i, with respect to time is determined by the differential change of the component mass flow along the axis of the column $\frac{\partial F_i^L}{\partial y}$ and the estimated component molar fluxes to and from the liquid bulk N_i. Molar fluxes are determined using the Maxwell-Stefan formulation in the liquid and vapour film models.

The change in energy holdup with respect to time, $\frac{dU}{dt}$, is determined by the differential change of 'energy flow' along the axis of the column, $\frac{\partial F_H^L}{\partial y}$ and the liquid heat fluxes at the liquid film-liquid bulk interface due to conduction, H_{liq}^{cond}, convection, H_{liq}^{conv} as well as the heat flux due to chemical absorption of CO_2, H_{abs}. Heat fluxes due to conduction and convection are accounted for in the film models.

Heat Loss (HL) = $\frac{131.64 \times Column\ Surface\ Area \times (T_{regen\_bottom} - T_{ambient})}{Height \times Cross\ Sectional\ Area \times NAE}$ (3)

The Heat Loss (HL) in the regenerator is calculated based on the temperature difference between the regenerator bottoms temperature (T_{regen_bottom}) and the ambient temperature ($T_{ambient}$). It is calculated per unit volume and distributed evenly along the axial length of the column by dividing by the Number of Axial Elements modelled in the column section (NAE). The constant value was derived from a correlation from the University of Texas at Austin test results [21].

Heat of absorption (or desorption): $H_{abs} = N_{CO_2} \cdot h_{abs}$ (4)

$$h_{abs} = R \cdot \left(-14281 - \left(\frac{1092554 \cdot \gamma^2}{T} \right) - \left(\frac{6800882 \cdot \gamma}{T} \right) + 32670.01 \cdot \gamma \right) \quad (5)$$

The specific heat of absorption, h_{abs}, was estimated based on the temperature, *T*, and the CO_2 loading of the solvent, γ. *R* is the universal gas constant [22].

The vapour bulk model has a similar structure to that of the liquid bulk model with the exception of the mass and energy accumulation terms which are assumed to be negligible in the vapour phase. At the interface between the liquid and vapour films, phase equilibrium is assumed to exist such that:

$$f_i^L \cdot x_i^{M,L} = f_i^V \cdot x_i^{M,V} \quad (6)$$

Phase equilibrium between liquid and vapour phases is assumed at the interface. The equilibrium molar compositions of the components in the vapour and liquid phases, x_i^M, are estimated based on the vapour and liquid fugacity coefficients, f_i.

2.3 Controllers for the process

Control schemes are illustrated in Figure 9. More details are presented in [11].

2.4 Model Validation at pilot plant scale

The steady-state validation of the chemical absorption plant model was carried out using data from one of the cases of the Separations Research Program at the University of Texas at Austin [21]. The absorber and regenerator columns of the pilot plant were both packed columns with diameters of 0.427m and total packing height of 6.1m. It is shown that the models give good predictions of the shape of the temperature profiles for both absorber and regenerator (referred to as the rate-based stand-alone model) [8]. Further validation studies have been carried out for the amine plant set-up (where the absorber and regenerator columns have been linked with recycle referred to as the rate-based integrated model) [10,11]. Validation results are shown for the absorber and regenerator in Figure 2.

The steady state predictions of the integrated model were found to be slightly better than the standalone models. In the latter, estimates of the input to the column had to be made and errors in such guesses would affect overall results. This suggests that the model predicts the interaction between the component parts of the plant (mainly the two columns) fairly well. It should be noted that the pilot plant in the study used to validate these results did not have a cross heat exchanger but used a combination of a heater and cooler [11]. Dynamic validation of the model could not be carried out because of the unavailability of dynamic plant test data.

2.5 Scale-up for Absorber and Stripper

Based on the experience gained from pilot plant studies and Chemical Engineering principles, the sizes, heat duties, configurations etc of the unit operations required to process the flue gas from a 500MWe subcritical power plant were determined. This design would also suffice for a 600MWe supercritical power plant which would have similar flue gas flows and composition. The system was designed to capture 90% of the CO_2 from 600kg/s of flue gas from the power plant using a 30wt% MEA solution. Preliminary design calculations were carried out with the following assumptions, providing the "Initial guess". The following assumptions were used:

a. Similar operating pressures for the absorber and regenerator used in the pilot plant study were used at full scale (1bar and 1.6bar respectively).
b. MEA solvent absorption capacity was assumed to be 0.18mol CO_2 / mol MEA which was used to calculate the solvent circulation rate.
c. All SO_2 and NOx have been removed from the flue gas stream
d. There is no water wash section in the absorber
e. Water balance is achieved using a water makeup control system

To process increased volumes of flue gas, the column diameters must be correspondingly increased. The approach used to determine the required column diameters of the absorber and the regenerator is described in Sections 2.5.1 and 2.5.2 respectively.

2.5.1 Number of Absorber columns and Absorber Diameter based on the generalized pressure drop correlation

Due to the structural limitations, [23] suggests that column diameters should not exceed 12.2m (40feet). To process the large volumes of flue gas from the power plant, more than one absorber column may be required. In addition, using more than one absorber column could help improve the turndown ratio of the process. Coal-fired power plants traditionally operate flexibly to meet varying demand. If such plants are fitted with post-combustion capture, it would be of advantage if they could continue to play such a role. The CO_2 capture process may therefore need to be designed to accommodate a large turndown ratio which would be easier to achieve with more than one column.

On the other hand, [3] reports that the absorber would most likely be the largest equipment in the capture plant since it would process huge volumes of flue gas. To provide a balance, therefore, the minimum number of columns required should be selected to keep capital costs down and minimize footprint requirements. The capacity of the absorber is largely based on its cross-sectional area. The column is usually designed to operate at the highest economical pressure drop to ensure good liquid and gas distribution [24].

The operating region of the packed column is limited by two main mechanisms: flooding and minimum liquid load [25]. Flooding sets the upper capacity of limit of the packed column. At this point, the pressure drop of the gas flow increases to an extent that the liquid is no longer able to flow downward against the gas flow [25]. The minimum liquid load refers to ensure lowest liquid flow rate sufficient mass transfer. Beyond this point, only a small proportion of the packing surface is wetted [25]. Figure 3 illustrates these limits.

The required solvent flow rate (liquid load) was estimated based on the estimates specified in Table 1.

[24] gives the recommended pressure drop per m packing for absorbers and strippers as 15 to 50mm of water per metre of packing height typically away from the flooding line (Figure 4). 42mm of water per metre of packing height was used for the design of both the absorber and stripper columns based on the recommendation of operating at the highest economical pressure drop [24].

F_{LV} is a flow parameter dependent on the L/G ratio of the column while K_4 is a modified gas load [25]. Based on the estimated F_{LV} flow parameter and the pressure drop parameter value chosen, the K_4 value is obtained from Figure 4.

$$K_4 = \frac{13.1(V_w^*)^2 \cdot F_p \cdot \left(\frac{\mu_L}{\rho_L}\right)^{0.1}}{\rho_v \cdot (\rho_L - \rho_v)} \quad (7)$$

μ_L = Liquid viscosity

F_p = Packing factor (dependent on the packing size and type)

The V_w* term is estimated from equation 7 and is then used to estimate the required cross sectional area of the column and thus the diameter. These values were used to estimate required column diameters for the process. The estimated absorber diameters required for 1 to 4 absorber columns in parallel are displayed in Figure 5.

From Figure 5, one absorber column would require a diameter of over 12m which would exceed 40feet. In addition, the turndown ratio of such a column may be significantly limited. Two or three columns could be selected with diameters of 9m and 7m respectively. For this study, a two-column absorber configuration was selected to minimize the footprint required for the columns. Selecting three or four columns may not provide significant returns in comparison with the large capital cost and footprint requirements this would demand.

2.5.2 Regenerator Diameter

Earlier simulation studies have shown that the regenerator processes much less volumetric vapour flow than the absorber; thus, a single column could be used. From the generalized pressure drop correlation method used above, the regenerator diameter was estimated as 8.39m, thus a single 9m diameter column would suffice.

It was impossible to validate the chemical absorption plant model at 500 MWe scale because no plant existed at the

time of this study. The summary of the specifications for the two columns in the CO_2 capture plant are shown in Table 2.

3. Subcritical coal-fired power plant model development and validation

Dynamic models for the furnace, boiler, 3-stage steam turbine, condenser and feed-water system were developed. The model was dynamically validated using plant data. The power plant model consists of various unit operations – including a furnace, various heaters, heat exchangers, pumps and a 3-stage turbine.

3.1 Model Development

The block flow diagram of the power plant model is shown in Figure 6.

3.1.1 Furnace model

Pulverized fuel (coal) is supplied to the furnace with the aid of primary air. The coal specification is given in Table 3. The furnace model includes only the air/gas side and as such it was assumed to be steady state since variables would adjust very quickly to any changes in inlet or boundary conditions. The overall heat balance is given in equation 8.

$$h_{in}m_{air,in} + h_{fuel}m_{fuel} + Q_{NCV}m_{fuel} = h_{out}m_{g,out} + h_{ash}m_{ash} + Q_{evap} + Q_{tfr} \quad (8)$$

The heat generated in the furnace by the combustion of pulverized fuel supplied at the fuel mass flow rate (fuel burn rate), m_{fuel}, is estimated based on the coal Net Calorific Value, Q_{NCV} . The heat generated in addition to the total enthalpy of the combustion air ($h_{in}m_{air,in}$) and fuel ($h_{fuel}m_{fuel}$) determine the total enthalpy of the outlet streams (flue gas and ash) as well as the heat transferred to the evaporative circuit, Q_{evap} and the thrown-forward radiation, Q_{tfr}. The air and gas enthalpies (h_{in} and h_{out}) are obtained from Multiflash physical property package that uses Lee-Kesler-Plöcker equation of state. To calculate Q_{evap} and Q_{tfr} it is necessary to calculate the adiabatic flame temperature. This is done from a heat balance equation similar to that given earlier, but with the outlet temperatures and enthalpies equal to the adiabatic flame temperature and with Q_{evap} and Q_{tfr} both equal to zero. An effective gas temperature is then found from the adiabatic and outlet temperatures:

$$T_{eff} = \beta T_{g,ad} + (1-\beta)T_{out} \quad (9)$$

Here, $T_{g,ad}$ is the adiabatic flame temperature and β is a user-input constant.

Then the evaporative heat is found based on κ_{evap}, a user-input constant; V_{furn}, the furnace volume; σ, the Stefan-Boltzman constant and $\rho_{g,out}$, the gas density at furnace outlet as shown in equation 10.

$$Q_{evap} = \frac{\kappa_{evap}V_{furn}\sigma(T_{eff})^4}{\rho_{g,out}} \quad (10)$$

The thrown-forward radiation, Q_{tfr}, is found from a similar equation; the only difference is the use of a different constant, κ_{tfr}.

3.1.2 Downcomer, Riser and Drum models

Heat generated in the furnace is transferred to the water walls (downcomer and risers), superheaters, reheaters and economisers. The mass flow rate of water in downcomer, $\dot{m}_{WDC}$ was modelled as proportional to the pressure drop in the downcomer [26].

$$\dot{m}_{WDC} = K_{DC}\sqrt{(P + \rho_{WDC} gZ - P_{DCB})\rho_{WDC}} \quad (11)$$

K_{DC} is an empirical constant that relates the pressure drop (estimated from the top (P) pressure, the hydrostatic pressure exerted by the water in the downcomer ($\rho_{WDC} gZ$) and the bottom downcomer pressure, P_{DCB}) and water density in downcomer, ρ_{WDC} to the mass flow rate.

Heat transfer is modelled in the riser section. The mass balance of fluid in the riser is given as [26]:

$$\dot{m}_{WDC} - \dot{m}_{WRO} = V_R \frac{d\rho_{WR}}{dt} \quad (12)$$

Enthalpy balance for water/steam in riser [26]:

$$V_R \frac{dh_{WR}}{dt} = Q_{WR} + \dot{m}_{WRO}(h_{WDC} - h_{WR}) \quad (13)$$

The heat transferred to the water in the riser tubes, Q_{WR} is given as

$$Q_{WR} = K_{WR} \cdot (T_{MR} - T_{WR})^3 \quad (14)$$

K_{WR} is an empirical constant that estimates the heat transfer based on the cube of the temperature difference between the riser tube walls (T_{MR}) and the steam temperature at the riser exit (T_{WR}). $\dot{m}_{WRO}$, the mass flow of water at riser exit is estimated in a similar manner to the $\dot{m}_{WDC}$ in equation 11

The fluid at the riser exit is a mixture of vapour and liquid phases. The fraction of liquid in the mixture entering the drum, XR is estimated based on the exit specific enthalpy (h_{WR}) and density (ρ_{WR}) based on the liquid and vapour specific enthalpies and densities.

Dynamic mass balance for steam in drum is [26]:

$$\dot{m}_{WRO} \cdot \mathrm{XR} - \dot{m}_{DO}^{V} = (V_{TD} - V_{WD}) \frac{d\rho_D^V}{dt} \quad (15)$$

This equation determines the mass flow of steam out of the drum, $\dot{m}_{DO}^{V}$. It is assumed that there is no heat loss from the drum to the surroundings.

Mass balance for water in drum is [26]:

$$\frac{dM_{WD}}{dt} = \dot{m}_{FW} + \dot{m}_{WRO}(1 - XR) - \dot{m}_{WDC} \quad (16)$$

$\dot{m}_{FW}$ is the mass flow of feed water into drum.

3.1.3 Heat exchanger-type models (Superheater and Reheater)

A transient heat exchanger model was used to model convective heat transfer in the superheater and reheater. The superheater platens and secondary superheater also accounted for radiative heat transfer. The model accounts for changes on the steam side as well as the gas side.

Mass balance for steam side

$$\dot{m}_{s,out} = \dot{m}_{s,in} - V_s \frac{d\rho_s}{dt} \quad (17)$$

Here, $\dot{m}_{s,out}$ and $\dot{m}_{s,in}$ are the mass flow rates of steam in and out of the tube. ρ_s is the steam density. V_s is the volume of steam in the tube.

Enthalpy balance for steam side (h_s)

$$\rho_s V_s \frac{dh_{s,out}}{dt} = m_{s,in} h_{s,in} - m_{s,out} h_{s,out} + U_s (T_w - T_{s,ave}) \quad (18)$$

Here, the overall admittance factor U_s is a function of the overall heat transfer coefficient. $T_{s,ave}$, is the average steam temperature.

Radiative heat transfer, q_{rad} is estimated based on the Stefan-Boltzmann law.

$$q_{rad} = \frac{K_{wall} V_g \cdot \sigma \cdot T^4}{\rho_g} \quad (19)$$

3.2 Important control systems

Superheater temperatures are controlled using spray water attemporators. These essentially mix the steam streams with controlled flows of spray water to achieve required temperatures. Reheater temperatures are controlled by using rear gas pass biasing dampers which control the flow of flue gas along the divided rear pass. The fuel burn rate and governor valve both control power plant power output. The target power plant output is directly controlled by the governor valve; this target also sets the target drum pressure. The drum pressure is controlled by the fuel burn rate.

3.3 Turbine models

These models apply generally to the High, Intermediate and Low Pressure turbines. The

Overall pressure ratio, *r*: governing their operation is given:

298 $$r = P_{out} / P_{in} \quad (20)$$

299 *3.4 Model Validation of power plant model*

300 The steady state results for the power plant model in gPROMS were validated on a steady state and dynamic basis.
301 The steady state model results were compared with the plant design data shows satisfactory agreement. Details of
302 the validation are discussed in [17]. It should be noted that recent plant data from Didcot suggests lower thermal
303 efficiency compared with design values [17].

304 The model was also validated against plant data. The plant data chosen for validation was as follows:

305 1. frequency-following operation at nominally 417 MW_e gross, 146 bar drum pressure
306 2. transient with the gross MW_e rising linearly to nominally 469 MW_e gross, 163 bar drum pressure
307 corresponding to an increase of 51 MW_e in 32 mins, ie 0.3% of full load per minute
308 3. frequency-following operation at nominally 469 MW_e gross, 163 bars drum pressure

309 A comparison between plant data and power plant model predictions for the transients is given in [17] showing that
310 the gPROMS model predicted flows fairly well through the course of the test.

311 **4. Linking the power plant model with the CO_2 capture model**

312 Three main links are included between the power plant and the CO_2 capture plant, as follows.

313 a. The flue gas stream which is to be processed.
314 b. The steam draw-off from the power plant to regenerate solvent in the reboiler
315 c. The condensate return from the reboiler to the power plant.

316 The linked power plant and CO_2 capture plant models is subsequently referred to as the whole plant model.

317 *4.1 Flue gas pre-processing*

318 Flue gas from the power plant must be cooled down to between 40 – 50°C for best absorption performance in the
319 absorber. Gases like sulphur oxides and nitrous oxides form heat stable salts with MEA solvent (which cannot be
320 regenerated). SO_2 concentrations of less than 10ppm are recommended. SO_2 removal is usually achieved in a Flue
321 Gas Desulphurization (FGD) unit. NOx is removed using Selective Catalytic Reduction (SCR), Selective
322 Noncatalytic Reduction (SCNR) or low NOx burners. Particulates in the flue gas could clog the column packings
323 and increase problems due to foaming. Particulate matter such as fly ash is removed by either electrostatic
324 precipitators or bag house filters.

In the whole plant model, it is assumed that all the SO_2 and NOx is removed upstream of the absorber and a Direct Contact Cooler (DCC) reduces the flue gas temperature to 40°C. All the particulate matter is assumed removed. In addition, the effect of oxygen in the degradation of MEA solvent is neglected. Thus oxygen is considered inert and its composition is simply incorporated in the nitrogen composition (Figure 7).

A blower adds the required head necessary to feed the flue gas to the absorber at just above atmospheric pressure. A splitter splits the flue gas flow into two equal streams that feed the two identical absorber columns as shown in Figure 7.

4.2 Steam draw-off

Steam is drawn off at the IP/LP crossover as recommended by [23] and [27] amongst other authors. Due to the reduced flow through the turbine, the pressure upstream the LP turbine drops with the draw-off as shown in Figure 8. This drop in pressure could be estimated by Stodola's Ellipse law [28]. The floating IP/LP crossover pressure configuration was employed [19,27]. This would accommodate a variable flow rate of steam draw-off. A throttling valve between the steam draw-off point and the LP turbine adds an additional pressure drop to raise the crossover pressure by about 1bar. This ensures that the pressure across the IP/LP crossover does not drop below the required pressure needed in the reboiler (at least 3bar). To employ this configuration, it is assumed that the IP turbine can accommodate the reduced exit pressures encountered with the steam draw-off [27].

A temperature controller measures the temperature of the lean solvent steam from the reboiler and controls the amount of steam drawn-off for regeneration using a control valve as shown in Figure 8. A water spray is used to cool down the steam temperature to just above saturation. It is assumed that there is no loss of total enthalpy in the process as the additional sensible heat was converted to latent heat of the vaporized spray water. This stream is then supplied to the reboiler where it exchanges heat with the solvent. It is assumed that all steam supplied condenses in the reboiler leaving saturated liquid condensate at the outlet. It is assumed that there are no heat losses and all the latent heat of vaporization is transferred to the reboiler fluid.

4.3 Condensate return

The condensate returned to the low pressure feedheater before being sent to the boiler feed pump. These two links between the power plant and CO_2 capture plant are shown in Figure 8.

4.4 Whole plant model topology

The whole plant model topology is shown in Figure 9.

5. Case Studies

Two steady state and two dynamic case studies are presented based on simulation results from the whole plant model described in Section 4:

Steady State Cases

- Plant performance with different absorber heights
- Plant performance with and without CO_2 capture and at different concentrations of MEA

Dynamic Cases

- Reducing power plant output
- Increasing Capture Level set point from 90% to 95%

5.1 Case Study 1 Increasing absorber packing height

Different packing heights of each of the absorber columns were tested to study the effect of increasing absorber packing height on the performance of the system. The parameter used to determine the effectiveness of each case was the heat requirement for CO_2 capture – the amount of heat required to separate 1kg of CO_2 from the flue gas mixture. The same design parameters summarized in Table 2 were used and absorber packing heights ranging from 17 to 37m were tested. [20] estimated that the absorber column design should be performed with a minimum height of 17m for the random packing IMTP50 packing considered. For each case, the capture level controller was set to capture 90% of the CO_2 in the flue gas. The results are presented in Figure 10. It is shown that significant savings of about 0.7MJ/kg CO_2 could be achieved whilst increasing absorber packing heights from 17 to 25m. There appears to be diminishing returns in the reduction in heat requirement over the range (which corresponds to the decrease in solvent circulation rates required to achieve 90% CO_2 capture). Relatively marginal savings could be achieved from 27m and above. There could be considerable operational savings with such packing heights that would compensate for the additional capital costs required.

5.2 Case Study 2 Plant performance with different concentrations of MEA

The whole plant performance with different concentrations of MEA is shown in Table 4 and compared to the base case without CO_2 capture. As discussed in Section 3.2, the fuel burn rate in the power plant is manipulated to control the drum pressure. The set point of the drum pressure is set to achieve a certain power output. In all cases presented in Table 4, the target power output was set to 500MW. However, due to the amount of steam drawn off for regeneration in the CO_2 capture cases, it was impossible to achieve the target and the actual power plant output depended on the amount of steam drawn off.

Power plant efficiency, η, is calculated as follows:

$$\eta = \frac{net\ power\ output}{fuel\ burn\ rate \times NCV} \quad (21)$$

The net power output was estimated by accounting for the power consumption of the various auxiliaries (estimated as 15MW). This power output corresponds to the electrical power generated.

With carbon capture, the power plant efficiency drops from 37.2% to the values given in Table 4 (it should be noted that the power requirement for CO_2 product compression is not considered in this study).

In summary, an increase in MEA concentration leads to easier CO_2 capture and less requirement for steam draw-off. The power plant efficiency is seen to increase with MEA concentration. For comparison, the fuel burn rate was set to a constant value of 56.8kg/s (which produced 500MW in the base case without capture) for all three cases. 30wt% MEA is typically employed in the chemical absorption process. 20wt% concentration would necessitate relatively higher solvent circulation rates which would increase the heat duty demanded by the reboiler to raise the temperature of the solvent circulated to the set point. On the other hand, this configuration required the least amount of pure MEA solvent (about 727kg/s) and at that concentration, would pose the least challenge in terms of corrosion. 40wt% MEA concentration would require the most solvent (1149kg/s compared to 912kg/s at 30wt%) and would have the most severe corrosion challenges. With increased MEA concentration, more heat of reaction is released whilst absorbing CO_2 with less solvent circulation. As a result, the absorber temperatures increase as shown in Table 4 and the efficiency of the absorption process thus reduces. Some savings could be achieved if temperatures are lowered in the column through techniques such as inter-cooling especially at higher concentrations of MEA solvent.

5.3 Case Study 3 – Reducing power plant output

This case simulates the effect of a decrease in power plant output over a period of 10 minutes. Power plant target output was ramped down from 440MW to 415MW over the aforementioned time period. The actual power plant power output is determined by the power plant power output controller which manipulates the fuel burn rate and governor valve opening to meet the target power output. The capture level controller set point was maintained at 90% CO_2 capture. Base case conditions were maintained for 4 hours before the disturbance was introduced. The whole plant model was then simulated for another 10 hours. Results of the simulation are shown in Figures 11 and 12.

Figure 11a shows the drop in actual power plant power output with time. The fuel burn rate is adjusted to achieve this drop (Figure 11b). With a reduced fuel burn rate, the flue gas produced reduces correspondingly and thus the flow of gas to the absorber column reduces. With less gas to process in the absorber, less solvent circulation is required (Figure 11d). The heat duty required in the reboiler to regenerate solvent thus decreases correspondingly

412 and there is therefore a reduced demand for steam from the power generation process (Figure 11c). The power plant
413 efficiency (Figure 11e) shows some initial perturbations before settling down to roughly the same steady state value.
414 The CO_2 capture level (Figure 11f) also oscillates and steadies out to the controller's set point of 90%.
415 Figure 12 shows the same results in terms of their percentage deviation from their original values (before the onset
416 of the disturbance). By mere observation, certain features become more apparent. For instance, the solvent
417 circulation rate shows the largest deviation perhaps because its settings provide tight control of the capture level –
418 from the same Figure, the capture level does not vary much. Even as such, there are periods where the capture level
419 is above the set point and more importantly below the set point as well. If emission regulations are such that the
420 capture level must not go below a certain value at any point in time, it is advisable to operate the capture plant
421 sufficiently above the minimum value so that disturbances from the power plant do not drop the capture level below
422 it. From Section 5.2, it is shown that achieving higher capture levels becomes increasingly difficult as 100% capture
423 is approached so care must be taken to select appropriate operating capture levels.
424 In addition, because of the tight controls on capture level and the resulting oscillations in solvent circulation rates,
425 the power plant power output oscillates in response to changing steam draw-off rates from the IP/LP crossover.
426 From Figure 11a and 12, the power plant output drops below the set point and takes a while to settle at the set point
427 making it difficult to achieve steady power output levels quickly. In this case, it appears that the tight control on
428 capture level is interfering with the power plant power output control.
429 The response of the power plant to operational changes is relatively fast. From the onset of the disturbance (reducing
430 the power plant output) the change in fuel burn rate and subsequently flue gas flow rate is relatively fast. In addition,
431 the capture level and solvent circulation rates also change soon after this disturbance is introduced. However, the
432 response of the amine plant is much slower. For instance, with a reduction in the solvent circulation rate, a lower
433 heat duty is demanded in the reboiler. However, from Figure 12, there is clearly a delay in the response of the steam
434 draw-off rate compared with that of the solvent circulation rate. This shows that the process dynamics of CO_2
435 capture plant is relatively slow response compared to that of the power plant. The manipulation of solvent
436 circulation rate (and subsequently steam draw-off rate) in turn imposes some disturbances on the power generation
437 process. It is therefore, not advisable to have such tight control on the capture level considering the interaction of
438 this control loop with the power plant power output control.
439 *5.4 Case study 4 – Increasing CO_2 capture level set point to 95%*
440 This case simulates the change in CO_2 capture level set point in the capture level controller from the base case value

of 90% to 95%. Power output targets were maintained. Base case conditions were maintained for 4 hours before the disturbance was introduced. The whole plant model was then simulated for another 10 hours. Results of the simulation are shown in Figures 13 and 14.

Figure 13a shows the power plant power output changes with time. Roughly, a 1.8% reduction in power plant output is observed after the disturbance (Figure 14). The fuel burn rate increases to compensate for the loss in power output (Figure 13b). It then steadies out at a slightly higher value than before the disturbance. Increasing the capture level set point would imply increased solvent circulation rates (Figure 13d). This increase attains a maximum of 34% (Figure 14) before it steadies out to almost 16% although the CO_2 capture level was increased by only 5% points (Figure 13f). This confirms that as 100% capture level is approached, CO_2 capture becomes increasingly difficult. This is clearly seen from Figure 14g where there is an increase in heat requirement for CO_2 capture after the disturbance was introduced. This value measures how much heat is required to separate 1kg of CO_2. It increases by just over 5% and appears to correspond to the increase in capture level at steady state (Figure 14).

The power plant efficiency reduces by almost 2.5% before attaining a steady state value 1.7% less than original due to the disturbance (Figure 13e and 14). From observing Figures 13c and 13e, it could be concluded that the efficiency reduction follows the response of the steam draw-off.

Both dynamic case studies show possible negative effects a poor control system or strategy could have on the integrated operation of a post combustion capture plant. Better process control could be achieved with improved controller tuning.

6. Conclusions

Dynamic models of the power plant and CO_2 capture plant have been developed, validated and linked. The scale-up of the CO_2 capture plant from pilot plant scale (where it was validated) to the scale required for processing flue gas from a 500MWe subcritical power plant was described. Four case studies were considered. The first involved investigating the whole plant performance with and without CO_2 capture. For the cases with CO_2 capture, 20, 30 and 40wt% MEA solution was utilized. The power plant efficiency was highest with the 40wt% case as expected and further improvements may be possible with the application of techniques such as inter-cooling. At such high solvent concentrations, more quantities of corrosion inhibitors would be required. From the investigations carried out, selecting 27m of absorber packing height offered a good balance between increasing column costs and reducing heat requirement in the reboiler. The two dynamic case studies showed that the CO_2 capture plant has a slower response than the power plant. Dynamic case studies reveal interaction of CO_2 capture level and power plant output control

loops. As the CO_2 capture level set point was increased from 90 to 95%, the thermal efficiency of the capture process reduced.

Acknowledgements

This work is partly funded by RWE npower and its support is greatly appreciated. The technical support from Process Systems Enterprise (PSE) Ltd, UK is also appreciated. The authors at Cranfield University would also like to acknowledge the financial support from Research Council UK Energy Programme (Ref: NE/H013865/1)

References

[1] Okuzumi N, Mitchell R. Current Status of MHI's CO_2 Recovery Technology and Road Map to Commercialization for Coal Fired Power Plant Application, International Conference & Exhibition: Nitrogen and Syngas, Bahrain, March 2010. www.mhi.co.jp/en/products/pdf/articles_07.pdf

[2] BERR. Advanced Power Plant Using High Efficiency Boiler/Turbine. Report BPB010. BERR (Department for Business Enterprise and Regulatory Reform); 2006. www.berr.gov.uk/files/file30703.pdf

[3] Abu-Zahra MRM, Schneiders LHJ, Niederer JPM, Feron PHM, Versteeg GF. CO_2 capture from power plants: Part I. A parametric study of the technical performance based on monoethanolamine. International Journal of Greenhouse Gas Control 2007; 1(1):37–46.

[4] Davidson R. Post-combustion carbon capture from coal fired plants – solvent scrubbing. Report CCC/125. IEA Clean Coal Centre; 2007. www.iea-coal.org.uk

[5] Davison J. Performance and costs of power plants with capture and storage of CO_2. Energy 2007; 32(7):1163–76.

[6] Herzog H, Meldon J, Hatton A. Advanced Post-Combustion CO_2 Capture. 2009. web.mit.edu/mitei/docs/reports/herzog-meldon-hatton.pdf

[7] Kvamsdal HM, Jakobsen JP, Hoff KA. Dynamic modelling and simulation of a CO_2 absorber column for post-combustion CO_2 capture. Chemical Engineering and Processing: Process Intensification 2009; 48(1):135-44.

[8] Lawal A, Wang M, Stephenson P, Yeung H. Dynamic modelling of CO_2 absorption for post-combustion capture in coal-fired power plants, Fuel 2009; 88, (12): 2455-62.

[9] Ziaii S, Rochelle GT, Edgar TF. Dynamic modeling to minimize energy use for CO_2 capture in power plants by aqueous monoethanolamine. Ind Eng Chem Res 2009; 48(13):6105–11.

[10] Lawal A, Wang, M, Stephenson P, Yeung H. Dynamic modeling and simulation of CO_2 chemical absorption process for coal-fired power plants, Computer Aided Chemical Engineering 2009; 27:1725-30.

[11] Lawal A, Wang M, Stephenson P, Koumpouras G, Yeung H. Dynamic Modelling and Analysis of Post-Combustion CO_2 Chemical Absorption Process for Coal-fired Power Plants, Fuel 2010; 89, (10): 2791–801.

[12] Lawal A, Wang M, Stephenson P. Investigating the dynamic response of CO_2 chemical absorption process in enhanced-O_2 coal power plant with post-combustion CO_2 capture, Energy Procedia 2010, In Press.

[13] Lu S. Dynamic modelling and simulation of power plant systems Proceedings of IMechE, Part A 1999; 213:7-22.

[14] Åström KJ, Bell RD. Drum boiler dynamics. Automatica 1999; 36, 363-78.

[15] Bhambare KS, Sushanta KM, Gaitonde UN. Modelling of coal fired natural circulation boiler. Transactions of ASME 2009; 129,159-66.

[16] Chaibakhsh A, Ghaffari A, Moosavian SAA. A simulated model for a once-through boiler by parameter adjustment based on genetic algorithms. Simulation Modelling Practice and Theory 2007; 15(9):1029-51.

[17] Stephenson P, Tian J, Jovanovic S, Tian X. Steady-state and dynamic modelling for a hybrid approach to post-combustion capture of carbon dioxide. In: Proceedings of the 12th IEA GHG Post-Combustion International Networking Meeting, University of Regina, Canada, September 2009.

[18] Aroonwilas A, Veawab A. Integration of CO_2 capture unit using single- and blended-amines into supercritical coal-fired power plants: Implications for emission and energy management. International Journal of Greenhouse Gas Control 2007; 1:143-150.

[19] Sanpasertparnich T, Idem R, Bolea I, deMontigny D, Tontiwachwuthikul P. Integration of post-combustion capture and storage into a pulverised coal-fired power plant, International Journal of Greenhouse Gas Control 2009, doi:10.1016/j.ijggc.2009.12.005.

519 [20] Cifre PG, Brechtel K, Hoch S, Garcia, H, Asprion N, Hasse H, Scheffknecht G. Integration of a chemical
520 process model in a power plant modelling tool for the simulation of an amine based CO_2 scrubber. Fuel 2009;
521 88(12): 2481-8.

522 [21] Dugas ER. Pilot plant study of carbon dioxide capture by aqueous monoethanolamine, M.S.E. Thesis,
523 University of Texas at Austin; 2006

524 [22] Oyenakan BA. Modeling of Strippers for CO_2 capture by Aqueous Amines. University of Texas at Austin; 2007

525 [23] Ramezan M, Skone TJ. Carbon dioxide capture from existing coal-fired power plants. Report DOE/NETL-
526 401/110907, National Energy Technology Laboratory (NETL); 2007.

527 [24] Sinnott RK. Chemical Engineering Design, 4th ed, Butterworth-Heinemann, Oxford, UK, 2005.

528 [25] Stichlmair JG, Fair JR. Distillation: Principles and Practices, Wiley-VCH, New York, 1998.

529 [26] Sidders JA. ANYDYM - a Fossil Fired Total Plant Model, Report PKR/SE/255, 1989.

530 [27] Lucquiaud M, Gibbins J. Retrofitting CO_2 capture ready fossil plants with post-combustion capture. Part 1:
531 requirements for supercritical pulverized coal plants using solvent-based flue gas scrubbing, Proceedings of the
532 Institution of Mechanical Engineers, Part A: Journal of Power and Energy 2009; 223(3):2041-967.

533 [28] Cooke DH. On prediction of off-design multistage turbine pressures by Stodola's Ellipse. Journal of
534 Engineering for Gas Turbines and Power 1985; 107(3):596-606.

Table1

Table 1 Calculation of required lean solvent flow

Description	Value
Flue gas mass flow rate (kg/s)	600
Flue gas mass composition (N_2)	0.748
Flue gas mass composition (CO_2)	0.209
Flue gas mass composition (H_2O)	0.042
Lean solvent mass fraction (MEA)	0.3048
Lean solvent mass fraction (CO_2)	0.0618
Lean solvent mass fraction (H_2O)	0.6334
Estimated required lean solvent mass flow (kg/s)	2900

Table2

Table 2 Summary of preliminary design parameters for chemical absorption plant

Description	Value
Design flue gas mass flow rate (kg/s)	600
CO_2 mass fraction in flue gas	0.21
CO_2 capture level (%)	90
Absorber Column Number	2
Absorber Diameter (m)	9
Absorber Height (m)	17
Regenerator Column Number	1
Regenerator Column Diameter (m)	9
Absorber operating pressure (10^5 Pa)	1.01
Regenerator operating pressure (10^5 Pa)	1.62
Lean solvent mass fraction (MEA)	0.3048
Lean solvent CO_2 loading (mol CO_2/mol MEA)	0.29

Table3

Table 3 Coal specification for power plant model

Composition % mass, as received basis	
Moisture	8
Ash	20
C	59.11
H	3.99
N	1
S	2.0
O	5.9
CV, MJ/kg, as received basis	
GCV	24.51
NCV	23.33

Table4

Table 4 Summary of parameters for the whole plant model with and without CO_2 capture and at different MEA concentrations

Description	**Without CO_2 Capture**	**With CO_2 Capture (20 wt% MEA)**	**With CO_2 Capture (30 wt% MEA)**	**With CO_2 Capture (40 wt% MEA)**
CO_2 capture level (%)	0	90	90	90
Solvent Circulation Rate (kg/s)	0	3663	3122	2964
Flue gas flow rate (kg/s)	589.6	589.6	589.6	589.6
Power Plant Output (MW)	500	437	453	467
Fuel burn rate (kg/s)	56.8	56.8	56.8	56.8
Power Plant efficiency	37.2	30.0	31.1	32
Steam draw-off flow rate (% of steam flow rate from IP turbine exit)	0	54	42	34
Maximum Absorber Temperature (K)	N/A	335	338	340

Figure1

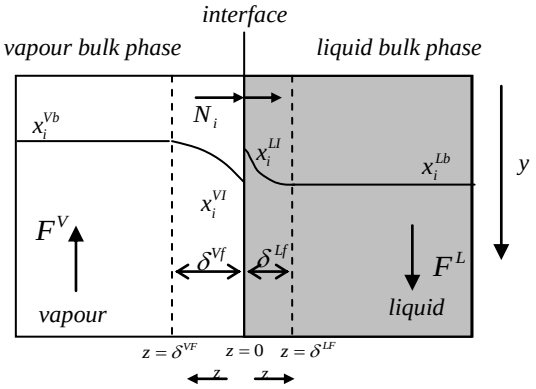

Figure 1 Liquid and vapour bulks, films and interface

Figure2

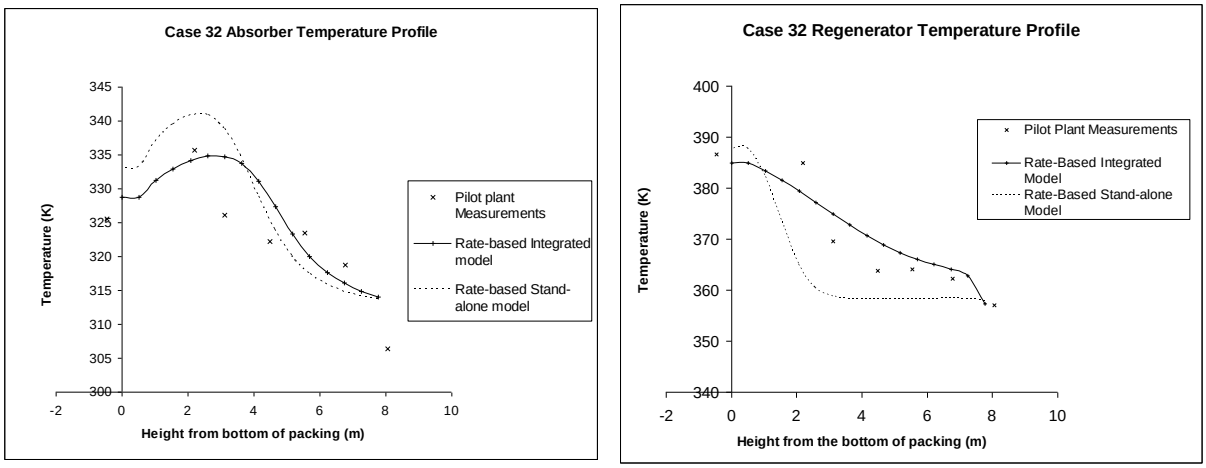

(a) (b)

Figure 2 (a) Absorber and (b) Regenerator temperature profile of columns for Case 32

Figure3

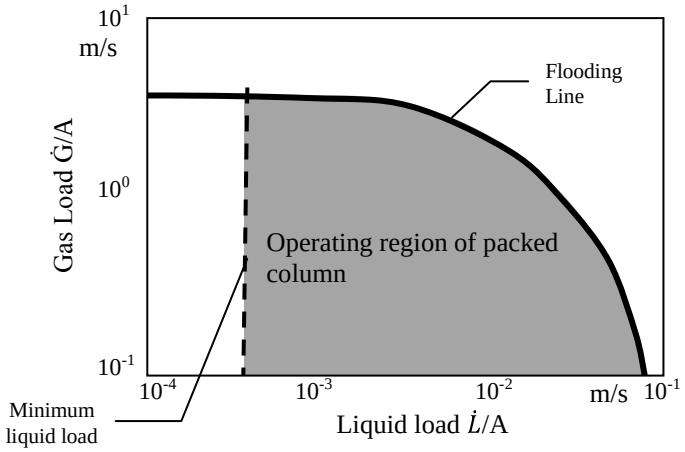

Figure 3 Operating region of a packed column adapted from [25]

Figure4

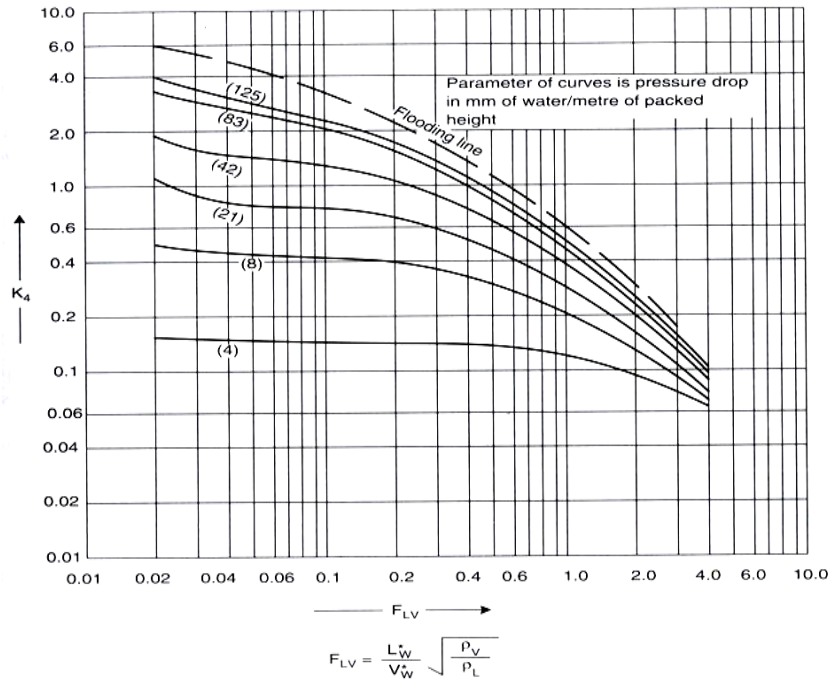

Figure 4 Generalized pressure drop correlation from [24]

Figure5

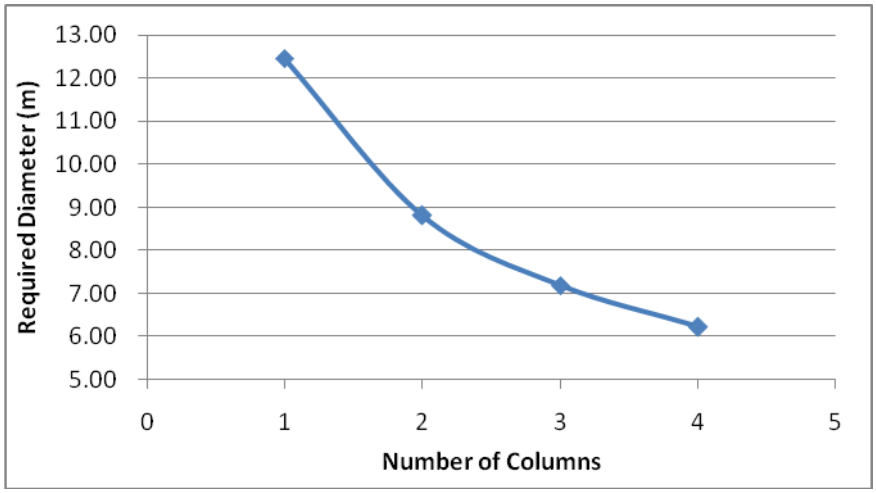

Figure 5 Required absorber diameter based on the number of absorber columns

Figure6

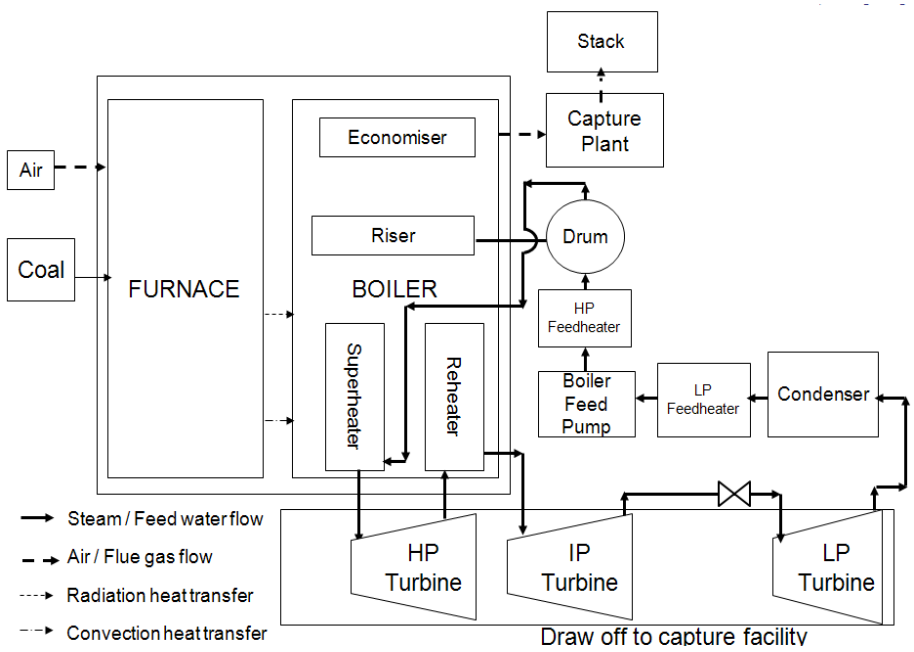

Figure 6 Power plant model block flow diagram

Figure7

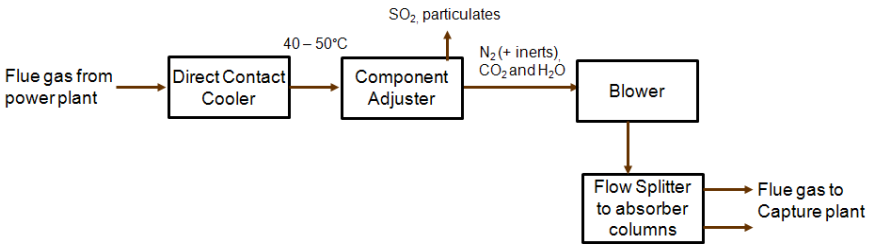

Figure 7 Linking the flue gas from the power plant with the CO_2 capture plant model

Figure8

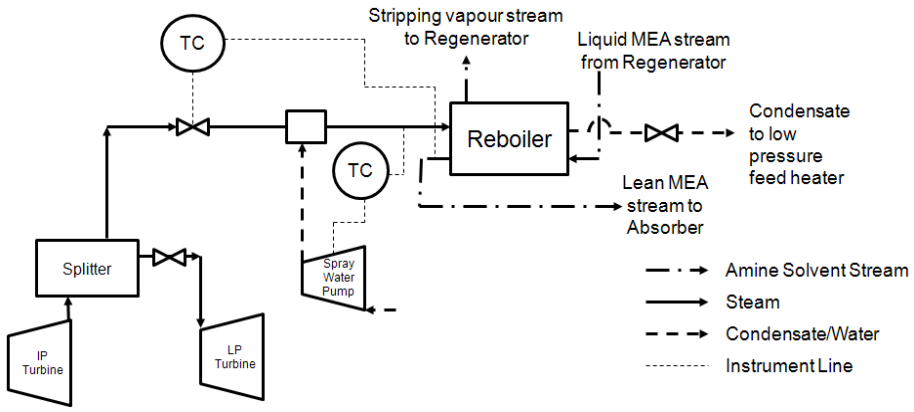

Figure 8 Steam draw-off and Condensate return

Figure9

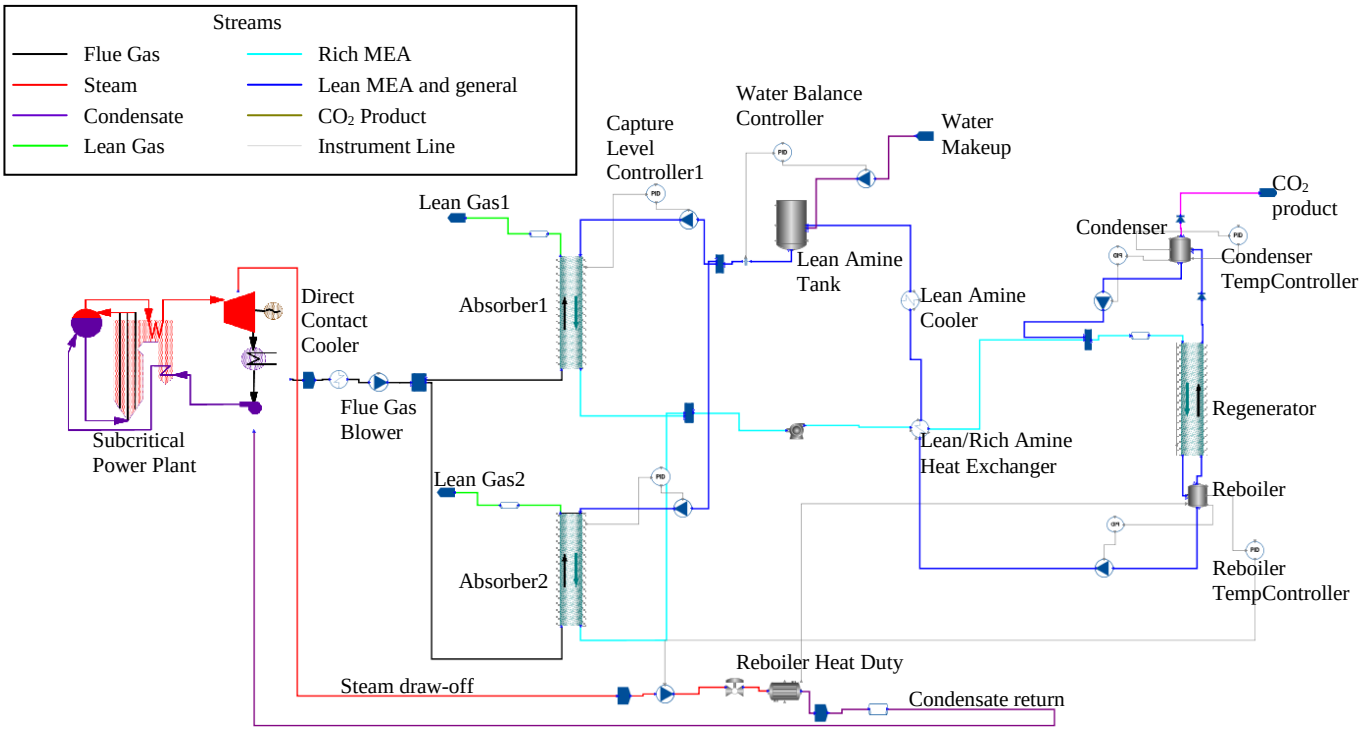

Figure 9 Whole Plant Model Topology

Figure10

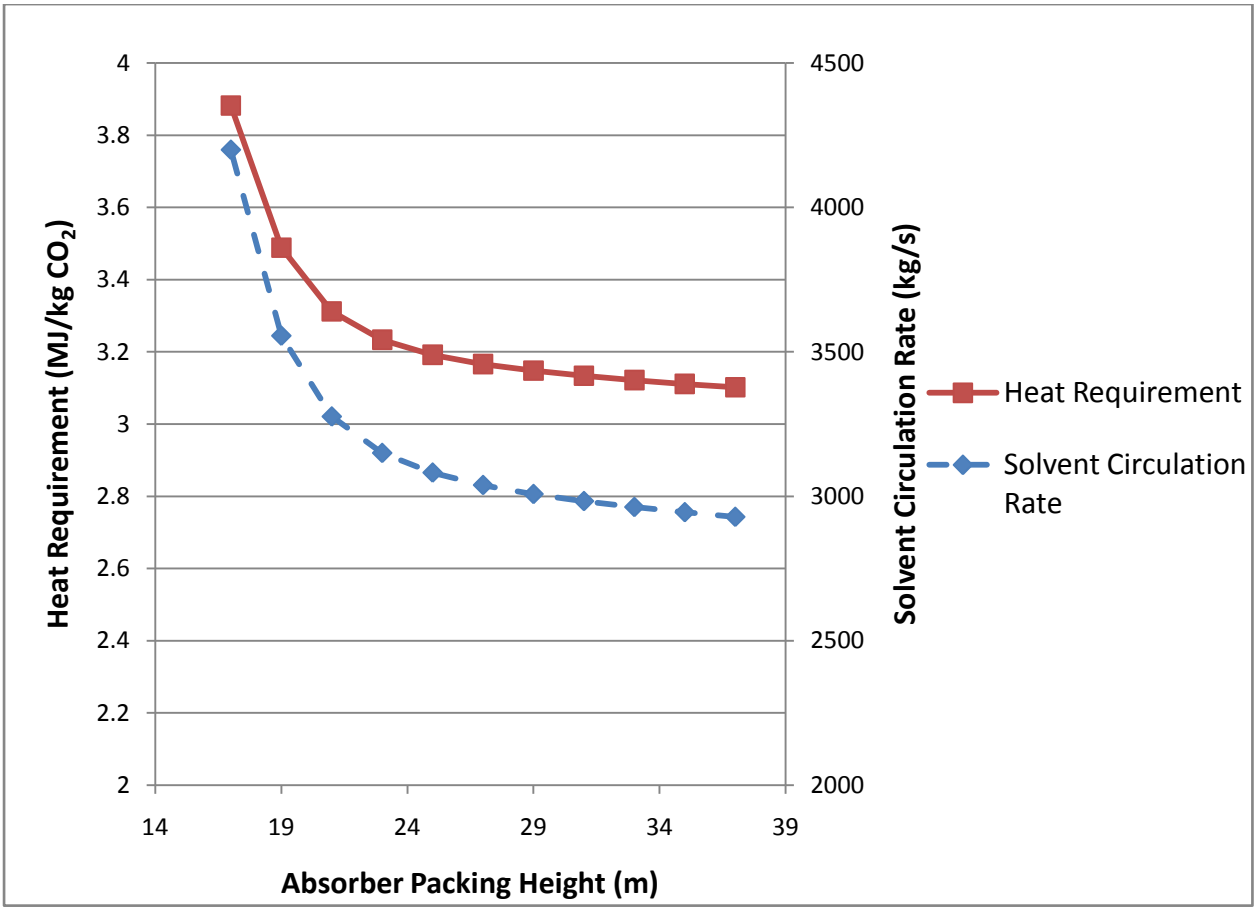

Figure 10 Plant performance with different Absorber packing heights

Figure11

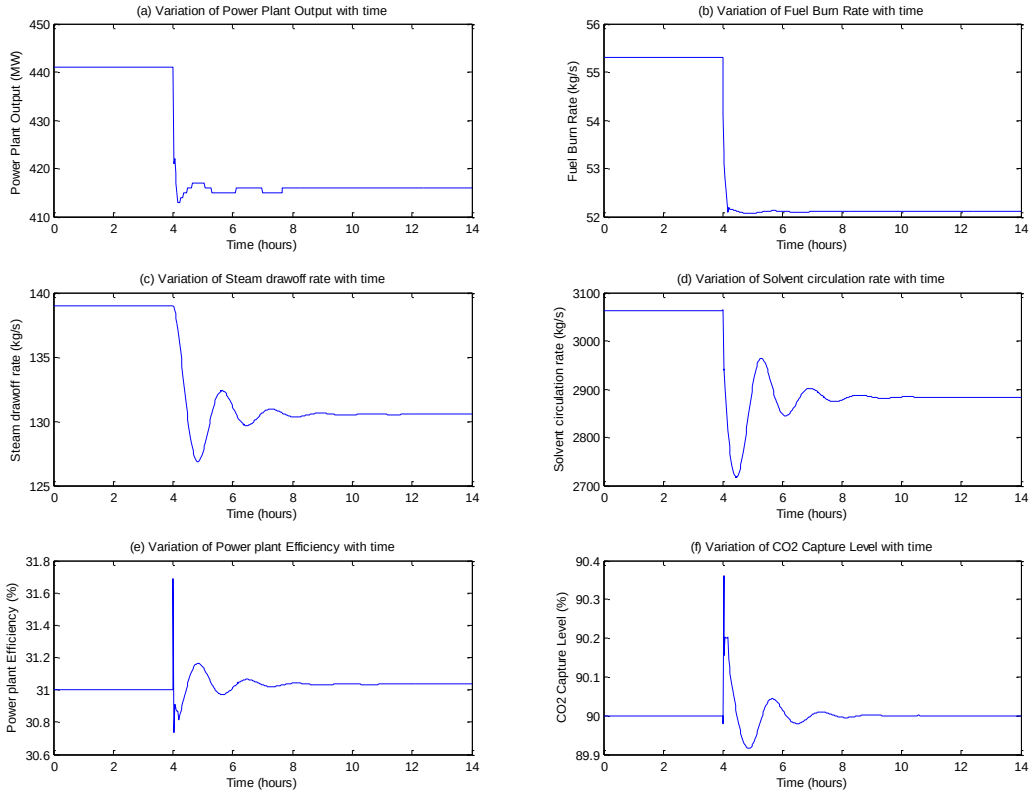

Figure 11 Effects of decreasing target power plant output

Figure12

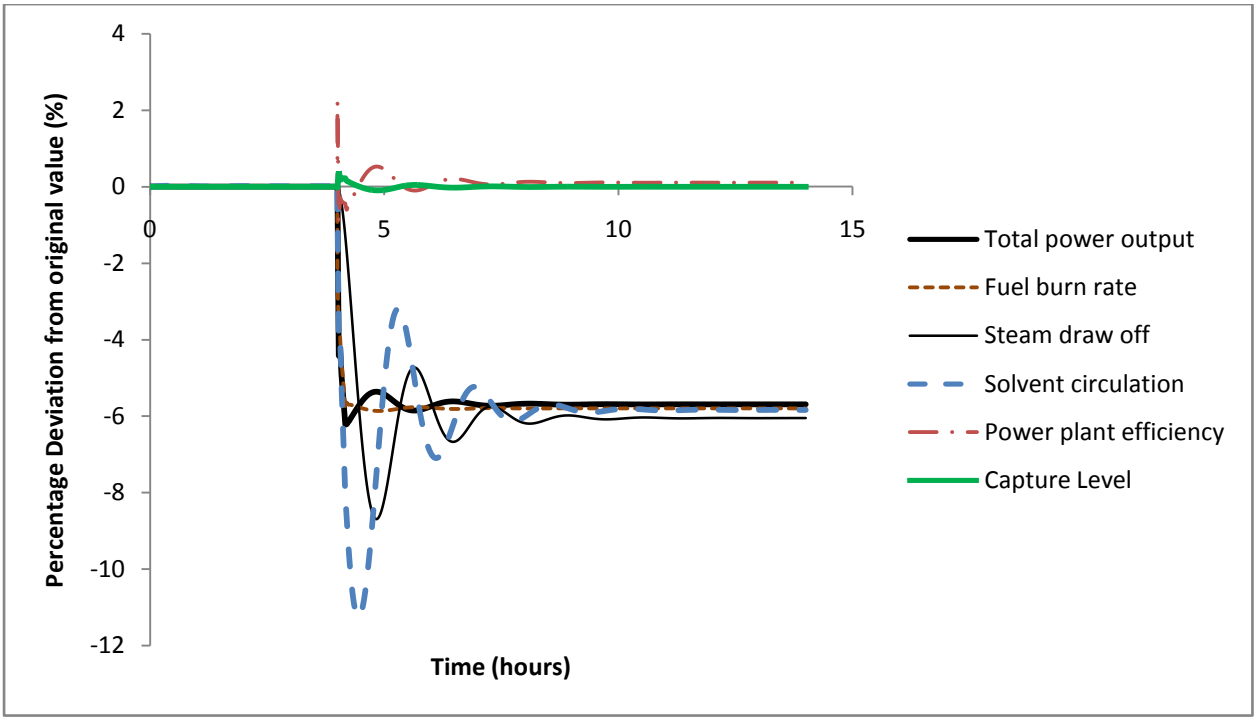

Figure 12 Percentage deviations with decreasing target power plant output

Figure13

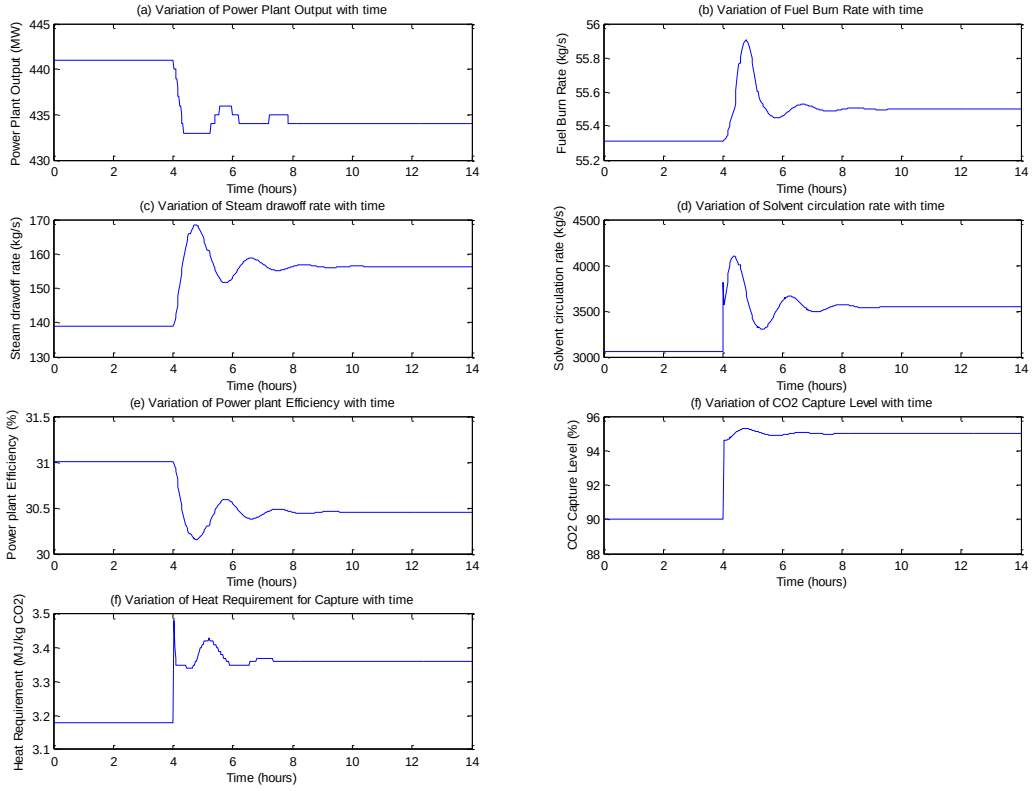

Figure 13 Effects of Increasing CO_2 Capture Level Set point

Figure14

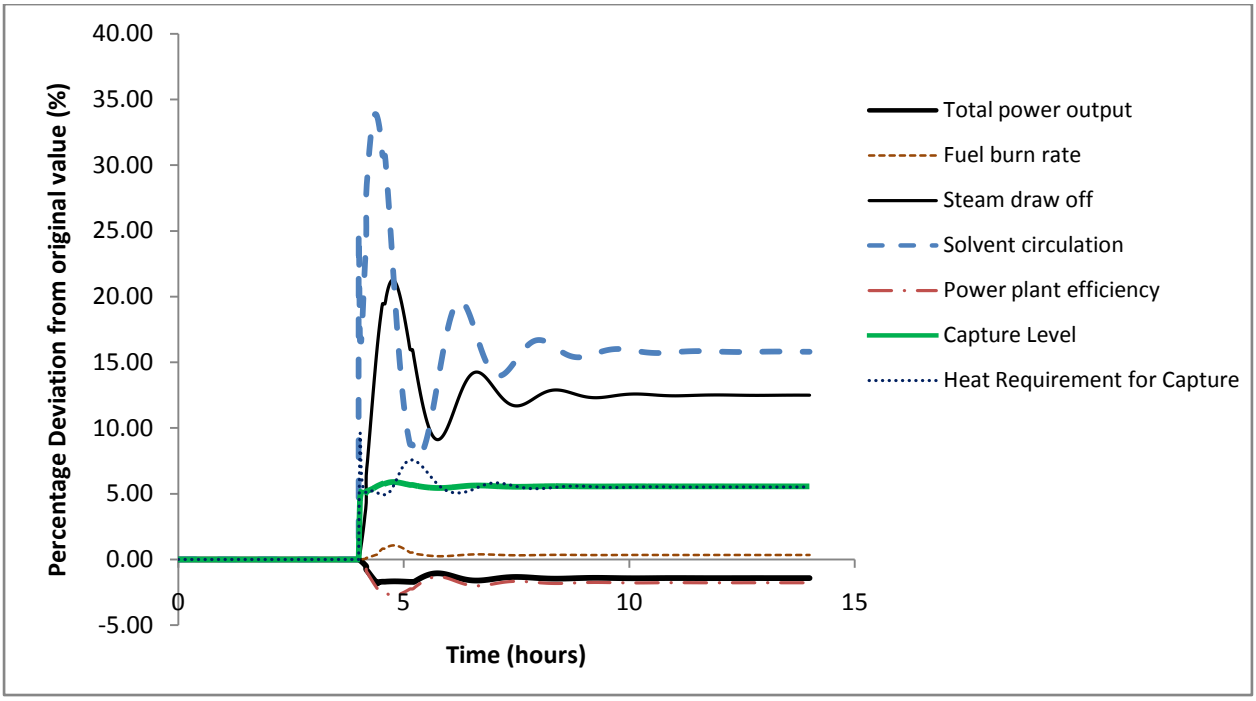

Figure 14 Percentage deviations with increasing CO_2 Capture Level Set point

Supplementary Material

Click here to download Supplementary Material: Nomenclature.docx